

Chapter 5

**Validation of Hammett's Linear Free
Energy Relationship Through Density
Functional Reactivity Theory**

5.1. Introduction:

In the previous chapter (chapter 4), a correlation was developed between equilibrium constant (K) and stabilization energy based on density functional reactivity theory (DFRT). The present chapter tries to validate Hammett's linear free energy relationship (LFER) through density functional reactivity theory (DFRT) based approach. Hammett equation is proposed for the first time through CDASE scheme based kinetic component and then tested on six different reactions. The study thus establishes that DFRT based energy component, $\Delta E_{B(A)}$ (which is very easy to compute) can be used, instead of k -(i.e., rate constant) values obtained either from experimental study or from computationally intensive conventional thermochemistry calculations, to generate reliable Hammett's plot.

It was Parr and Pearson¹ who first formulated analytical expression of stabilization energy and the amount of electron transfer associated with the electron transfer interaction between the two species using chemical potential equalization principle.²⁻⁴ For reactions involving reacting species of comparable sizes, Roy and collaborators⁵ re-denoted the stabilization energy expression proposed by Parr and Pearson and extended it further to propose an energy decomposition scheme known as CDASE (i.e., Comprehensive Decomposition Analysis of Stabilization Energy). Subsequently, the CDASE scheme was exploited to explain kinetics and thermodynamics of different types of chemical and biological interactions.⁶⁻¹¹

CDASE scheme was further extended by Hamid *et al.*¹² after including the perturbation on external potential of the interacting species (thoroughly discussed in chapter 2) On the basis of this extended formalism, a presumption, regarding the effect of solvent polarity on stabilization energy, was made. Further, a new thermodynamic parameter was introduced which was termed as the 'net desolvation energy'. The 'net desolvation energy' turned out to be the 'negative of free energy of solvation'¹³ (thoroughly discussed in chapter 3). Recently, a relation between equilibrium constant (K) and DFRT based stabilization for a related series of reactions was developed by Hamid and Roy¹⁴ (thoroughly discussed in chapter 4).

In organic chemistry, a lot of bimolecular reactions proceed via transition state leading to more than one final product. The rates of such reactions vary from reaction to reaction and depend primarily on two factors and these are (i) the type of reaction and (ii) type of substituents on the reactants for a particular type of reaction. Hammett equation¹⁵ is one of the fundamental equations that relates thermodynamic and kinetic parameters of related series of reactions in the spirit of

linear free energy relationship (LFER)¹⁶⁻²⁰ using two reaction parameters i.e., (i) substituent constant (σ)^{19, 21} and (ii) reaction constant (ρ).²¹

In the spirit of Hammett's linear free energy relationship the thermodynamics of a reaction (say, R₁) can be correlated with the kinetics of a related reaction (say, R₂) having same substituent (say X) through the following equations:

$$\left(\log \frac{K_X}{K_H}\right)_{R_1} = \rho_1 \sigma \quad (5.1)$$

$$\left(\log \frac{k_X}{k_H}\right)_{R_2} = \rho_2 \sigma \quad (5.2)$$

Combining equations (5.1) and (5.2), we can write,

$$\left(\log \frac{k_X}{k_H}\right)_{R_2} = \frac{\rho_2}{\rho_1} \left(\log \frac{K_X}{K_H}\right)_{R_1} \quad (5.3)$$

where, K_H = equilibrium constant for unsubstituted reactant in reaction 1

K_X = equilibrium constant when H is substituted by the group (or atom) X in the reaction 1.

k_H = rate constant when the reactant is unsubstituted in reaction 2

k_X = rate constant when the reactant is substituted by the group (or atom) X in reaction 2

ρ_1 = reaction constant for reaction 1

ρ_2 = reaction constant for reaction 2

σ = substituent constant (for H atom, $\sigma = 0$)

The physical significance of equation (5.3) is that if reactions R₁ and R₂ are of similar type (i.e., they follow similar type of reaction mechanism) a plot of $\log \frac{k_X}{k_H}$ of reaction R₂ vs. $\log \frac{K_X}{K_H}$ of reaction R₁ will be linear and the slope will give ratio of the reaction constant values of the two reactions (i.e., ρ_2/ρ_1).

However, for a particular reaction (say R₁) it can be written,

$$\left(\log \frac{k_X}{k_H}\right)_{R_1} = \rho_1 \sigma = \left(\log \frac{K_X}{K_H}\right)_{R_1} \quad (5.4)$$

or,

$$\left(\log \frac{k_X}{k_H}\right)_{R_1} \propto \left(\log \frac{K_X}{K_H}\right)_{R_1} \quad (5.5)$$

The Hammett substituent constant (σ) was originally based on benzoic acid (with different substitution in *meta* and *para* position) ionization in water and hence susceptible to be affected by solvation changes. Hence, a modified set of substituent constants (denoted as σ^0), developed after averaging over many reactions and so expected to better express universal substituent character, was proposed and found to be more reliable.²² With this modified substituent constants the Hammett equation can be re-written as,

$$\log \frac{k_X}{k_H} = \rho^0 \sigma^0 \quad (5.6)$$

Thus, a plot of either $\log \frac{k_X}{k_H}$ vs. σ or $\log \frac{k_X}{k_H}$ vs. σ^0 for any reaction should be linear and the slope will provide the reaction constant, ρ (or ρ^0). Here it should be noted that the above relations [equations (5.4) and (5.6)] are valid only for *meta* and *para*-substituents. The reasons for this is that for *meta* and *para*-substituted isomers the changes in rate constant (k) or equilibrium constant (K) (and so ΔG^\ddagger or ΔG) are predominantly changes in ΔH^\ddagger (activation enthalpy) or ΔH (reaction enthalpy) since substituents do not affect much the ΔS . However, for *ortho* substituents the ΔS value is affected differently in different reactions as well as in different solvents.

As the CDASE-scheme based stabilization energy can be decomposed into the kinetic and thermodynamic components, in principle, these can be used to verify the Hammett equation [i.e., equation (5.4) or (5.6)]. Thus, the theme of the present study is to test whether the kinetic component of stabilization energy [$\Delta E_{B(A)}$] can be used, instead of k , to validate equations (5.4) or (5.6) (i.e., the LFER as envisaged by Hammett).

This chapter is designed as per the following sections: In section 5.2 (a), a theoretical background of the CDASE scheme is provided with the definitions of kinetic and thermodynamic components of stabilization energy. In section 5.2 (b), Hammett equation, in the form of CDASE-scheme based kinetic energy components, is formulated. Section 5.3 covers computational details. Results and discussions are elaborated in section 5.4. Finally, in the concluding section (section 5.5), the entire study is summarized.

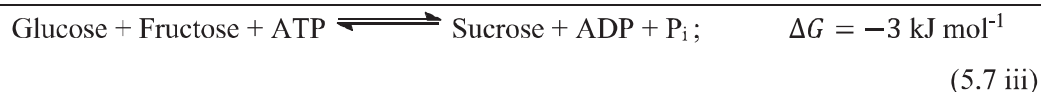
5.2. Theoretical background:

(a) DFRT based reactivity descriptors:

In the process of a chemical reaction, electron transfer from one system to the other [i.e., from the electron donor (B) to the electron acceptor (A)] results in change in the overall energy of the combined system, which can be termed as ‘stabilization energy’ (ΔE_{SE}). The expression of this stabilization energy, by summing up the energy changes of the individual species, was first formulated by Parr and Pearson¹ in terms of global reactivity descriptors. [equation (1.46)].

As mentioned in the introductory section (section 5.1), Roy and collaborators⁵ re-denoted the energy expression of the individual species as shown in chapter 1 [equations (1.49) and (1.50)]. These expressions represent the kinetic and thermodynamic components of the stabilization energy of the CDASE scheme.⁵ A careful analysis reveals that $\Delta E_{B(A)}$ is a positive quantity and is defined as ‘internal assistance’ to overcome the activation barrier (rather than the activation barrier itself). This is the energy acquired by the combined system by virtue of their electronic properties. On the other hand, $\Delta E_{A(B)}$ is a negative quantity and more negative is its value more is the stability of the final adduct or products. The net energy change is given by sum of equations (1.49) and (1.50) and is represented by equation (1.48).

The electron donation by a Lewis base and the acceptance by a Lewis acid can be considered as a coupled process similar to a pair of coupled reactions. In a coupled reaction the energy demand of the endergonic one is met by that of the exergonic one having more negative reaction Gibbs’ energy. Thus the overall coupled reaction will have negative reaction Gibbs’ energy. One typical example is the biochemical reaction as shown below:



In case of the coupled process of electron donation by a Lewis base and acceptance by a Lewis acid, the former will be an endergonic [$\Delta E_{B(A)}$] and the later one will be an exergonic process [$\Delta E_{A(B)}$]. The quantities $\Delta E_{B(A)}$ and $\Delta E_{A(B)}$ depends on the electronic properties (e.g., IP, EA, etc.) of both B and A. These are denoted by equations (1.15) and (1.20a).

Although, higher ΔG value in reaction (5.7 i) apparently indicates an unfavorable thermodynamic situation regarding the feasibility of this step [i.e., reaction (5.7 i)], it will indicate a favorable situation if ΔG value [i.e., ΔG of reaction (5.7 iii)] is negative. Thus, the validity of the statement ‘higher is the $\Delta E_{B(A)}$ value, higher is the rate’ stems from the fact that the positive value of $\Delta E_{B(A)}$ is compensated partly by higher negative value of $\Delta E_{A(B)}$ and finally producing net negative $\Delta E_{SE(AB)}$ value.

The amount of electron transfer from the donor to the acceptor is given by equation (1.47). The computation of two global reactivity descriptors i.e., electronic chemical potential (μ)^{1,4,23} and chemical hardness (η)^{1,23,24} of both A and B are required for the calculation of $\Delta E_{B(A)}$, $\Delta E_{A(B)}$, $\Delta E_{SE(AB)}$ and ΔN . Analytically, chemical potential and chemical hardness are defined as: $\mu = \left(\frac{\partial E}{\partial N}\right)_v$ and $\eta = \left(\frac{\partial^2 E}{\partial N^2}\right)_v$ (here, v is external potential, i.e., potential due to positions of the nuclei, plus any other external potential, if present). The working equations of these two quantities are given by equations (1.15) and (1.20a), respectively.

(b) Hammett equation in the form of CDASE-scheme based kinetic energy components:

As interpreted in section 5.2(a) the kinetic energy component [$\Delta E_{B(A)}$] [equation (1.49)] is a positive valued quantity and higher its value higher is the rate of the reaction. Thus, in principle, the Hammett equation can be re-written as,

$$\log \frac{[\Delta E_{B(A)}]_X}{[\Delta E_{B(A)}]_H} = \rho\sigma \text{ (or } \rho^0\sigma^0\text{)} \quad (5.8)$$

So, a linear plot of $\log \frac{[\Delta E_{B(A)}]_X}{[\Delta E_{B(A)}]_H}$ vs. σ (or σ^0) with reasonably high correlation coefficient (R^2) will demonstrate the reliability of theoretically generated $\Delta E_{B(A)}$ values (instead of experimentally obtained k - values, as is done conventionally) in validating Hammett’s LFER.

From equation (5.8) it is obvious that $\Delta E_{B(A)}$ [equation (1.49)] and $\Delta E_{A(B)}$ [equation (1.50)] are analytically related to each other. Hence, we can write,

$$\frac{[\Delta E_{A(B)}]_X}{[\Delta E_{A(B)}]_H} = \frac{[\Delta E_{SE(AB)}]_X - [\Delta E_{B(A)}]_X}{[\Delta E_{SE(AB)}]_H - [\Delta E_{B(A)}]_H} \quad (5.9)$$

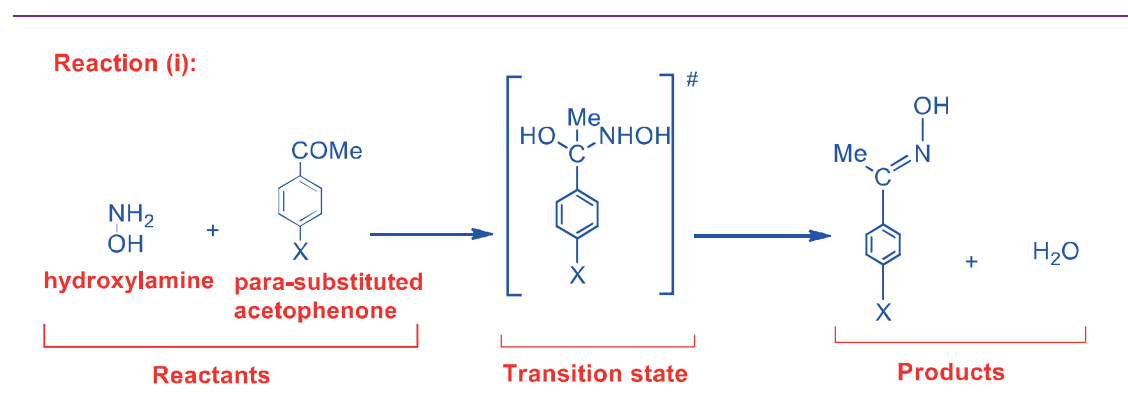
Hence, the plots of $\log \frac{[\Delta E_{A(B)}]_X}{[\Delta E_{A(B)}]_H}$ vs. $\rho\sigma$ (or $\rho^0\sigma^0$) and $\log \frac{[\Delta E_{B(A)}]_X}{[\Delta E_{B(A)}]_H}$ vs. $\rho\sigma$ (or $\rho^0\sigma^0$) for different X will be qualitatively of similar type having very close R^2 values. In fact this is aligned to the spirit of LFER, which states that reactions which are thermodynamically favorable are also

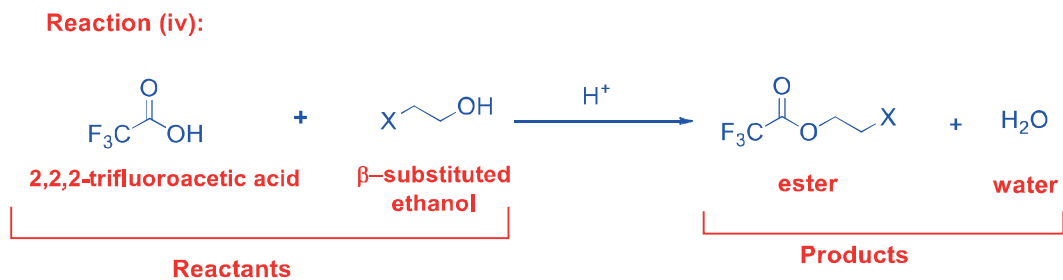
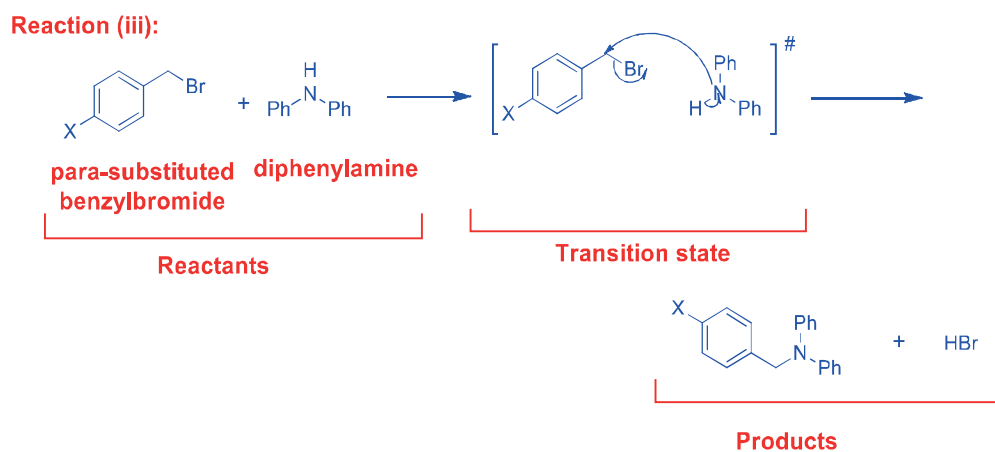
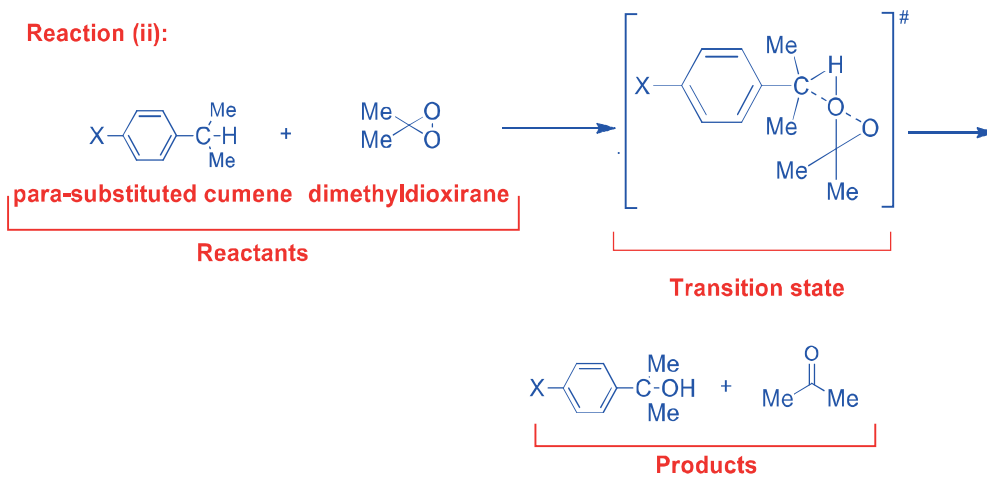
kinetically favorable as in case of CDASE scheme $\Delta E_{B(A)}$ represents the kinetic aspect and $\Delta E_{A(B)}$ represents the thermodynamic aspect of a chemical interaction.

Also, stabilization energy and binding energy (conventional) represent the same physical property. e.g., the energy released when chemical species interact with each other forming an adduct. Hence equation (5.9) is, in principle, valid for binding energy as well. Again, as bond dissociation energy (BDE) is negative of binding energy the above argument should be valid for BDE also.

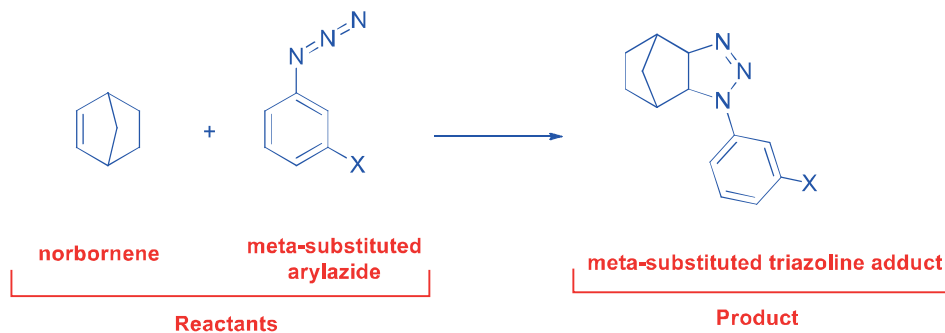
5.3. Computational Details:

The representative reactions, to plot $\log \frac{[\Delta E_{B(A)}]_X}{[\Delta E_{B(A)}]_H}$ vs. σ (or σ^0) chosen are: (i) reaction of para-substituted acetophenones with hydroxylamine²⁵ in ethanol, (ii) reaction of para-substituted cumenes with dimethyldioxirane²⁶ in acetone, (iii) reaction of para-substituted benzylbromides with diphenylamine²⁷ in methanol, (iv) reaction of 2,2,2-trifluoroacetic acid with β -substituted ethanol,²⁸ (v) reaction of norbornene with meta-substituted arylazide in ethylacetate²⁹ and (vi) reaction of norbornene with para-substituted arylazide in ethylacetate.²⁹ Computations are carried out in same solvents in which corresponding experimental studies are conducted. The schematic diagrams representing reactions (i) – (vi) are shown in Figure 5.1.

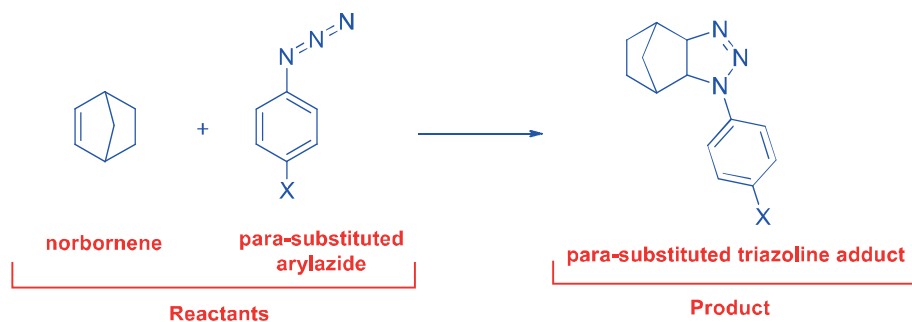




Reaction (v):



Reaction (vi):



where, -Me = $-\text{CH}_3$ group, -Ph = $-\text{C}_6\text{H}_5$ group, -X = substituent on one of the reactants.

Figure 5.1. Schematic diagrams representing reactions of (i) para-substituted acetophenones with hydroxylamine, (ii) para-substituted cumenes with dimethyldioxirane, (iii) para-substituted benzylbromides with diphenylamine, (iv) 2,2,2-trifluoroacetic acid with β -substituted ethanol, (v) norbornene with meta-substituted arylazide and (vi) norbornene with para-substituted arylazide.

Geometry optimizations of all the reactant structures followed by frequency calculations (in order to confirm that no imaginary frequency is present) are carried out using Gaussian09 program package.³⁰ For computation of $\Delta E_{B(A)}$ values [equation(1.49)], single point energy calculations of all the neutral reactants and the corresponding monocationic and monoanionic species are carried out. For the ionic species optimized geometries of the neutral systems are considered (as IP and EA values have to be vertical). Optimizations and single point energy calculations are carried out at two different levels of theory: (i) B3LYP^{31,32}/6-31G(d,p),³³ LANL2DZ and (ii) M06-2X³⁴/6-31G(d,p),³³ LANL2DZ. The LANL2DZ basis set with ECP^{35,36}

is used for those atoms with higher atomic numbers [e.g., I atom in reaction (ii)]. The choice of using two different functionals (i.e., B3LYP and M06-2X) in the present cases is to test the consistency (and hence, the reliability) of the generated data through CDASE scheme. Also, M06-2X functional is known to take care of dispersion corrections reasonably well.³⁷ The effect of solvent is taken care implicitly (both for geometry optimization as well as computation of reactivity indices) using IEF-PCM^{38,39} solvation model.

5.4. Results and Discussion:

Analysis of generated data for reactions (i) – (vi) and thus validation of DFRT based Hammett equation [equation (5.8)] is discussed below:

(a) Validation of DFRT based Hammett equation [equation (5.8)] for reaction (i):

Table 5.1(a) represents the values of $\Delta E_{B(A)}$, $\Delta E_{A(B)}$ and $\Delta E_{SE(AB)}$ for the reaction of para-substituted acetophenone with hydroxylamine calculated in both the chosen methods. The substituents (-X) on para-substituted acetophenone and the corresponding Hammett substituent constants (σ) are also shown. Table 5.1(b) represents the corresponding values of $\log \frac{[\Delta E_{B(A)}]_X}{[\Delta E_{B(A)}]_H}$. It is to be noted here that para-substituted acetophenones act as electron acceptors (A), whereas hydroxylamine acts as an electron donor (B) in all the cases. This is confirmed from the positive values of ΔN [computed through equation (1.47)] in all the cases [section 5.2 (a) for details] as shown in Table 5.1 (c).

Table 5.1 (a). The values of $\Delta E_{B(A)}$, $\Delta E_{A(B)}$ and $\Delta E_{SE(AB)}$ (in kcal mol⁻¹) for the reaction of para-substituted acetophenones with hydroxylamine in ethanol at B3LYP/6-31G(d,p) and M06-2X/6-31G(d,p) levels of theory. -X is the substituent on the para-position of acetophenone.

Entry	-X	σ	B3LYP/6-31G(d,p)			M06-2X/6-31G(d,p)		
			$\Delta E_{B(A)}$	$\Delta E_{A(B)}$	$\Delta E_{SE(AB)}$	$\Delta E_{B(A)}$	$\Delta E_{A(B)}$	$\Delta E_{SE(AB)}$
1	-OCH ₃	-0.27	9.35	-10.70	-1.35	13.60	-16.25	-2.65
2	-C ₂ H ₅	-0.15	12.80	-15.22	-2.42	14.01	-17.02	-3.01
3	-H	0.00	14.35	-17.33	-2.98	16.00	-19.85	-3.85
4	-Br	0.23	15.22	-18.44	-3.22	16.97	-21.15	-4.18
5	-NO ₂	0.78	26.82	-35.00	-8.18	33.80	-47.83	-14.03

Table 5.1 (b). The values of $\log \frac{[\Delta E_{B(A)}]_X}{[\Delta E_{B(A)}]_H}$ for the reaction of para-substituted acetophenones with hydroxylamine in ethanol at B3LYP/6-31G(d,p) and M06-2X/6-31G(d,p) levels of theory. -X is the substituent on the para-position of acetophenone.

Entry	-X	σ	$\log \frac{[\Delta E_{B(A)}]_X}{[\Delta E_{B(A)}]_H}$	
			B3LYP/6-31G(d,p)	M06-2X/6-31G(d,p)
1	-OCH ₃	-0.27	-0.186	-0.070
2	-C ₂ H ₅	-0.15	-0.049	-0.057
3	-H	0.00	0.000	0.000
4	-Br	0.23	0.025	0.025
5	-NO ₂	0.78	0.272	0.324

Table 5.1 (c). The values of charge transfer (ΔN) for the reaction of para-substituted acetophenones with hydroxylamine in ethanol at B3LYP/6-31G(d,p) and M06-2X/6-31G(d,p) levels of theory. -X is the substituent on the para-position of acetophenone. In all the cases with the substituents as shown, para-substituted acetophenone acts as an electron acceptor (A) and hydroxylamine acts as an electron donor (B).

Entry	-X	σ	ΔN	
			B3LYP/6-31G(d,p)	M06-2X/6-31G(d,p)
1	-OCH ₃	-0.27	0.13	0.17
2	-C ₂ H ₅	-0.15	0.17	0.18
3	-H	0.00	0.18	0.2
4	-Br	0.23	0.19	0.22
5	-NO ₂	0.78	0.32	0.40

From Table 5.1 (a), it is easy to explain that when the H-atom in the para-position of acetophenone is substituted by electron donating groups (EDGs) like -OCH₃ and -C₂H₅, the corresponding $\Delta E_{B(A)}$ values are less positive and $\Delta E_{SE(AB)}$ values are less negative as compared to unsubstituted acetophenone. This is because of the fact that the EDGs increase the electron density in the ring, which in turn decreases electron accepting ability of the -COCH₃ group. On the other hand, when the para-position of acetophenone is substituted by electron withdrawing

groups (EWGs) like -Br and -NO₂, the corresponding $\Delta E_{B(A)}$ become more positive and $\Delta E_{SE(AB)}$ become more negative when compared to the unsubstituted acetophenone. This is because EWGs decrease the electron density in the molecule which in turn increases its electron accepting ability. The corresponding plots of $\log \frac{[\Delta E_{B(A)}]_X}{[\Delta E_{B(A)}]_H}$ vs. σ for the reaction of para-substituted acetophenones with hydroxylamine are shown in Figure 5.2.

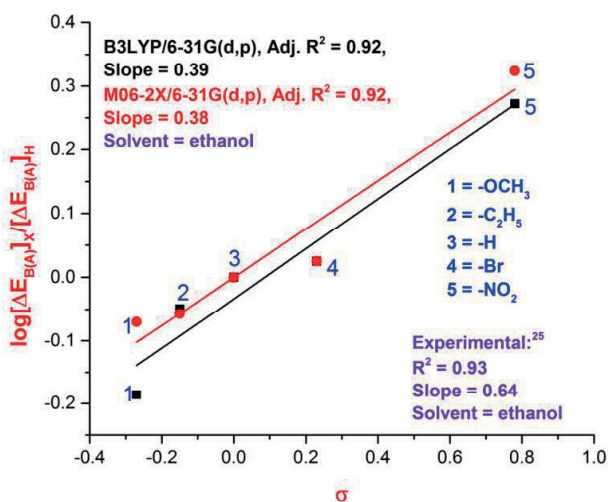


Figure 5.2. Plot of $\log \frac{[\Delta E_{B(A)}]_X}{[\Delta E_{B(A)}]_H}$ vs. σ for the reaction of para-substituted acetophenones with hydroxylamine at B3LYP/6-31G(d,p) and M06-2X/6-31G(d,p) levels of theory.

The plots clearly establish the electrophilic nature of the substituted acetophenones in the reaction. This is obvious from the positive values of the slopes [0.39 in B3LYP/6-31G(d,p) and 0.38 in M06-2X/6-31G(d,p) methods] indicating that reaction constant ρ is positive. The correlation co-efficient is reasonably high ($R^2 = 0.92$) and almost same as experimentally generated one.²⁵ The corresponding plots using Exner's substituent constant values (i.e., σ^0) are shown in Figure 5.3 [the corresponding values of σ^0 and $\log \frac{[\Delta E_{B(A)}]_X}{[\Delta E_{B(A)}]_H}$ are shown in Table 5.1 (d)].

It is gratifying to note that the values of ρ^0 are again positive here although difference in R^2 values is higher between the two methods.

Table 5.1 (d). The values of σ^0 for different substituents and $\log \frac{[\Delta E_{B(A)}]_X}{[\Delta E_{B(A)}]_H}$ values for the reaction of para-substituted acetophenones with hydroxylamine in ethanol at B3LYP/6-31G(d,p) and M06-2X/6-31G(d,p) levels of theory. -X is the substituent on the para-position of acetophenone.

Entry	Substituent (-X)	σ^0	$\log \frac{[\Delta E_{B(A)}]_X}{[\Delta E_{B(A)}]_H}$	
			B3LYP/6-31G(d,p)	M06-2X/6-31G(d,p)
1	-OCH ₃	-0.12	-0.186	-0.070
2	-C ₂ H ₅	-0.15	-0.049	-0.057
3	-H	0.00	0.000	0.000
4	-Br	0.26	0.025	0.025
5	-NO ₂	0.81	0.272	0.324

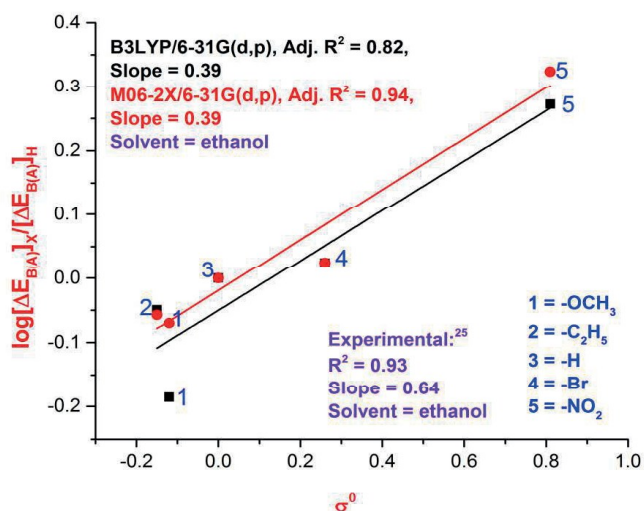


Figure 5.3. Plot of $\log \frac{[\Delta E_{B(A)}]_X}{[\Delta E_{B(A)}]_H}$ vs. σ^0 for the reaction of para-substituted acetophenones with hydroxylamine at B3LYP/6-31G(d,p) and M06-2X/6-31G(d,p) levels of theory.

(b) Validation of DFRT based Hammett equation [equation (5.8)] for reaction (ii):

Table 5.2 (a) represents the values of $\Delta E_{B(A)}$, $\Delta E_{A(B)}$ and $\Delta E_{SE(AB)}$ for the reaction of para-substituted cumene with dimethyldioxirane. The substituents (-X) and the corresponding Hammett

substituent constant (σ) values of the para-substituted cumenes are also shown. Table 5.2 (b) contains the values of $\log \frac{[\Delta E_{B(A)}]_X}{[\Delta E_{B(A)}]_H}$ for the same reaction. Para-substituted cumene acts as an electron donor when the substituents are -OH, -OC₆H₅, -OCH₃, -CH₃, -H, -I, whereas dimethyldioxirane acts as an electron acceptor (A). However, when the substituent in para-position is -COCH₃ cumene behaves as an electron acceptor and dimethyldioxirane acts as an electron donor. This is confirmed from the positive values of ΔN in all the cases except when the substituent on cumene is -COCH₃. In the later reaction ΔN became positive only when p-COCH₃ cumene is assumed to be an electron acceptor (A) and dimethyldioxirane as an electron donor (i.e., B) in equation (1.47) [Table 5.2 (c)].

Table 5.2 (a). The values of $\Delta E_{B(A)}$, $\Delta E_{A(B)}$ and $\Delta E_{SE(AB)}$ (in kcal mol⁻¹) for the reaction of para-substituted cumenes with dimethyldioxirane in acetone at B3LYP/6-31G(d,p), LANL2DZ (for I atom) and M06-2X/6-31G(d,p), LANL2DZ (for I atom) levels of theory.-X is the substituent on the para-position of cumene.

Entry	-X	σ	B3LYP/6-31G(d,p),			M06-2X/6-31G(d,p),		
			LANL2DZ (for I atom)			LANL2DZ (for I atom)		
			$\Delta E_{B(A)}$	$\Delta E_{A(B)}$	$\Delta E_{SE(AB)}$	$\Delta E_{B(A)}$	$\Delta E_{A(B)}$	$\Delta E_{SE(AB)}$
1	-OH	-0.37	10.83	-12.54	-1.71	7.40	-8.18	-0.78
2	-OC ₆ H ₅	-0.32	9.65	-10.87	-1.22	6.55	-6.85	-0.30
3	-OCH ₃	-0.27	11.22	-13.07	-1.85	7.60	-8.50	-0.90
4	-CH ₃	-0.17	9.41	-10.65	-1.24	6.40	-6.90	-0.50
5	-H	0.00	7.88	-8.70	-0.82	4.65	-4.90	-0.25
6	-I	0.18	3.65	-3.80	-0.15	3.50	-3.70	-0.20
7	-COCH ₃	0.50	1.798	-1.83	-0.032	2.74	-2.96	-0.22

Table 5.2 (b). The values of $\log \frac{[\Delta E_{B(A)}]_X}{[\Delta E_{B(A)}]_H}$ for the reaction of para-substituted cumenes with dimethyldioxirane in acetone at B3LYP/6-31G(d,p), LANL2DZ (for I atom) and M06-2X/6-31G(d,p), LANL2DZ (for I atom) levels of theory. -X is the substituent on the para-position of acetophenone.

Entry	-X	σ	$\log \frac{[\Delta E_{B(A)}]_X}{[\Delta E_{B(A)}]_H}$	
			B3LYP/6-31G(d,p), LANL2DZ (for I atom)	M06-2X/6-31G(d,p), LANL2DZ (for I atom)
1	-OH	-0.37	0.138	0.202
2	-OC ₆ H ₅	-0.32	0.088	0.148
3	-OCH ₃	-0.27	0.153	0.213
4	-CH ₃	-0.17	0.077	0.138
5	-H	0.00	0.000	0.000
6	-I	0.18	-0.334	-0.123
7	-COCH ₃	0.50	-0.642	-0.231

Table 5.2 (c). The values of charge transfer (ΔN) for the reaction of para-substituted cumenes with dimethyldioxirane in acetone at B3LYP/6-31G(d,p), LANL2DZ (for I atom) and M06-2X/6-31G(d,p), LANL2DZ (for I atom) levels of theory. -X is the substituent on the para-position of cumene. Dimethyldioxirane acts as an electron acceptor (A) and para-substituted cumene acts as an electron donor (B) when the substituents (-X) are from entry 1 to entry 6. When the substituent (-X) on para-position of cumene is -COCH₃, it acts as an electron acceptor (A).

Entry	-X	σ	ΔN	
			B3LYP/6-31G(d,p), LANL2DZ (for I atom)	M06-2X/6-31G(d,p), LANL2DZ (for I atom)
1	-OH	-0.37	0.14	0.09
2	-OC ₆ H ₅	-0.32	0.12	0.07
3	-OCH ₃	-0.27	0.15	0.09
4	-CH ₃	-0.17	0.12	0.07
5	-H	0.00	0.09	0.05
6	-I	0.18	0.04	0.04
7	-COCH ₃	0.50	0.02*	0.05*

*Positive ΔN values are generated when p-COCH₃-C₆H₄-CH-(CH₃)₂ is assumed to be A and (CH₃)₂C(O)₂ as B [equation (1.47)].

Here, it should be noted that -I substituted cumene should not be considered for correlation analysis as the basis set used for I is LANL2DZ, which is different from 6-31G(d,p) used for other atoms. The negative value of $\log \frac{[\Delta E_{B(A)}]_X}{[\Delta E_{B(A)}]_H}$ clearly shows that presence of -I and -COCH₃ in para-position of cumene retard the rate of the reaction when compared to unsubstituted cumene. The same is observed in the experimental study also.²⁶ Moreover, the value of ρ is negative in both the methods when either Hammett's parameter (σ) or Exner's parameter (σ^0) is used for plotting (Figures 5.4 below and 5.5). The values of σ^0 and $\log \frac{[\Delta E_{B(A)}]_X}{[\Delta E_{B(A)}]_H}$ are shown in Table 5.2 (d).

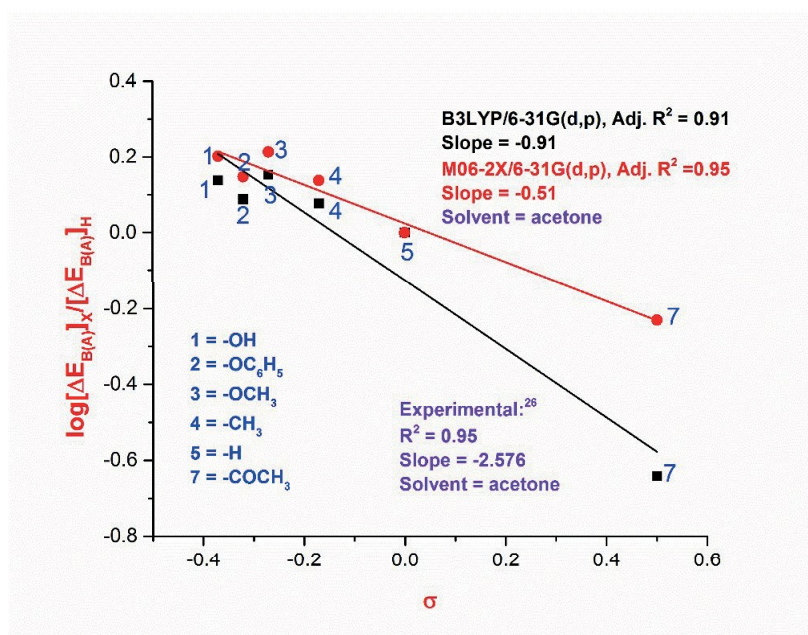


Figure 5.4. Plot of $\log \frac{[\Delta E_{B(A)}]_X}{[\Delta E_{B(A)}]_H}$ vs. σ for the reaction of para-substituted cumenes with dimethyldioxirane at B3LYP/6-31G(d,p) and M06-2X/6-31G(d,p) levels of theory.

Table 5.2 (d). The values of σ^0 for different substituents and $\log \frac{[\Delta E_{B(A)}]_X}{[\Delta E_{B(A)}]_H}$ values for the reaction of para-substituted cumenes with dimethyldioxirane in acetone at B3LYP/6-31G(d,p), LANL2DZ (for I atom) and M06-2X/6-31G(d,p), LANL2DZ (for I atom) levels of theory. -X is the substituent on the para-position of cumene.

Entry	Substituent (-X)	σ^0	$\log \frac{[\Delta E_{B(A)}]_X}{[\Delta E_{B(A)}]_H}$	
			B3LYP/6-31G(d,p), LANL2DZ (for I atom)	M06-2X/6-31G(d,p), LANL2DZ (for I atom)
1	-OH	-0.22	0.138	0.202
2	-OC ₆ H ₅	0.05	0.088	0.148
3	-OCH ₃	-0.12	0.153	0.213
4	-CH ₃	-0.14	0.077	0.138
5	-H	0.00	0.000	0.000
6	-I	0.28	-0.334	-0.123
7	-COCH ₃	0.47	-0.642	-0.231

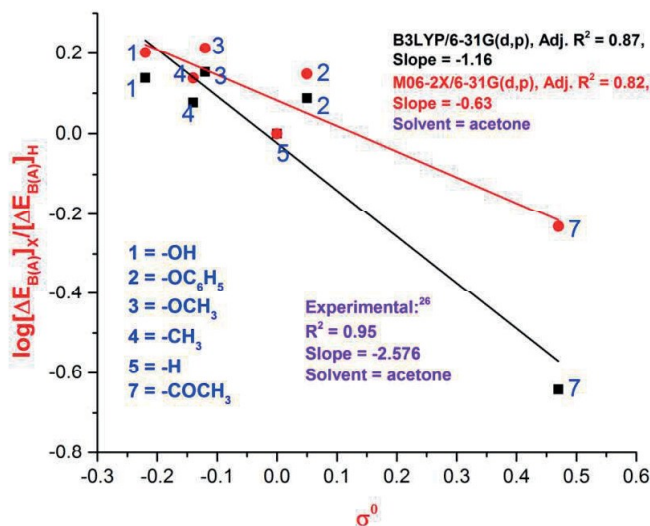


Figure 5.5. Plot of $\log \frac{[\Delta E_{B(A)}]_X}{[\Delta E_{B(A)}]_H}$ vs. σ^0 for the reaction of para-substituted cumenes with dimethyldioxirane in ethanol at B3LYP/6-31G(d,p) and M06-2X/6-31G(d,p) levels of theory.

The negative value of ρ is indicative of the fact that the reaction is accelerated by electron donating substituents, unlike ionization of benzoic acid, where electron donating substituents on the benzene ring retards the reaction rate. In case of ionization of benzoic acid, electron density of the aromatic ring in the transition state increases (because the H^+ leaves the electron on the $C_6H_5CO_2^-$ moiety) and hence electron withdrawing substituents increase the rate of dissociation reaction. In the present case electron-donating substituents meet the electron demand of the electron deficient transition state. As the scale of ρ is established with respect to benzoic acid ionization, the value is negative in the present case. It is obvious that the slopes differ much when the plots are generated by the two computational methods as well as from experimental one. One of the probable reasons for this difference (between the plots generated from two computational methods) is the difference of the functionals used. M06-2X functional is known to take care of dispersion interaction and ionic hydrogen bonding interactions in much better way than B3LYP functional.³⁷ As the extent of these two types of interactions differ reasonably among the chosen systems the difference of energy component $\Delta E_{B(A)}$ also shoots up. Also, the experimental data are generated at room temperature, whereas the theoretical calculations are carried out at 0 K. The temperature effect on reactivity differs significantly from system to system, which computational methods could not take care. This is probably the reason of the high slope of the plot generated from experimental data.

(c) Validation of DFRT based Hammett equation [equation (5.8)] for reaction (iii):

Table 5.3 (a) represents the values of $\Delta E_{B(A)}$, $\Delta E_{A(B)}$ and $\Delta E_{SE(AB)}$ for the reaction of para-substituted benzylbromide with diphenylamine. The substituents (-X) on the para position and the corresponding Hammett substituent constants (σ) are also shown. Table 5.3 (b) contains the values of $\log \frac{[\Delta E_{B(A)}]_X}{[\Delta E_{B(A)}]_H}$ for the same reaction. The generated positive ΔN values [Table 5.3 (c)] in all the cases and in both the methods confirm the claim that para-substituted benzylbromides behave as electrophile (i.e., electron acceptor, A) and diphenylamine act as nucleophile (i.e., electron donor, B) in the reaction.

Table 5.3 (a). The values of $\Delta E_{B(A)}$, $\Delta E_{A(B)}$ and $\Delta E_{SE(AB)}$ (in kcal mol⁻¹) for the reaction of para-substituted benzylbromide with diphenylamine in methanol at B3LYP/6-31G(d,p) and M06-2X/6-31G(d,p) levels of theory. Here, -X is the substituent on the para-position of benzylbromide.

Entry	-X	σ	B3LYP/6-31G(d,p)			M06-2X/6-31G(d,p)		
			$\Delta E_{B(A)}$	$\Delta E_{A(B)}$	$\Delta E_{SE(AB)}$	$\Delta E_{B(A)}$	$\Delta E_{A(B)}$	$\Delta E_{SE(AB)}$
1	-CH ₃	-0.17	12.30	-14.90	-2.60	12.95	-15.10	-2.15
2	-H	0.00	14.10	-17.00	-2.90	14.90	-17.71	-2.81
3	-Br	0.23	20.87	-24.32	-3.45	22.35	-25.90	-3.55
4	-NO ₂	0.78	37.20	-50.40	-13.20	40.99	-58.41	-17.42

Table 5.3 (b). The values of $\log \frac{[\Delta E_{B(A)}]_X}{[\Delta E_{B(A)}]_H}$ for the reaction of para-substituted benzylbromide with diphenylamine in methanol at B3LYP/6-31G(d,p) and M06-2X/6-31G(d,p) levels of theory. Here, -X is the substituent on the para-position of benzylbromide.

Entry	-X	σ	$\log \frac{[\Delta E_{B(A)}]_X}{[\Delta E_{B(A)}]_H}$	
			B3LYP/6-31G(d,p)	M06-2X/6-31G(d,p)
			1	-CH ₃
2	-H	0.00	0.000	0.000
3	-Br	0.23	0.170	0.176
4	-NO ₂	0.78	0.421	0.439

Table 5.3 (c). The values of charge transfer (ΔN) for the reaction of para-substituted benzylbromides with diphenylamine in methanol at B3LYP/6-31G(d,p) and M06-2X/6-31G(d,p) levels of theory. Here, -X is the substituent on the para-position of benzylbromide. In all the cases with the substituents as shown, para-substituted benzylbromide acts as an electron acceptor (A) and diphenylamine acts as an electron donor (B).

Entry	-X	σ	ΔN	
			B3LYP/6-31G(d,p)	M06-2X/6-31G(d,p)
1	-CH ₃	-0.17	0.22	0.18
2	-H	0.00	0.17	0.21
3	-Br	0.23	0.25	0.23
4	-NO ₂	0.78	0.48	0.50

Regarding the effect exerted by different substituents on the reactivity, it is obvious that EDG retards the rate [negative value of $\log \frac{[\Delta E_{B(A)}]_{CH_3}}{[\Delta E_{B(A)}]_H}$ for $-CH_3$ substituted benzylbromide, Table 5.3(b)] whereas EWGs accelerate the rate when compared to the unsubstituted benzyl bromide. The observation is similar when universal substituent constant (σ^0) is used for plotting [Table 5.3(d) and Figure 5.7]. The electrophilic nature of substituted benzylbromide is also obvious from the plot of $\log \frac{[\Delta E_{B(A)}]_X}{[\Delta E_{B(A)}]_H}$ vs. σ (Figure 5.6), as in both the methods ρ turns out to be positive with reasonably good correlation coefficient values.

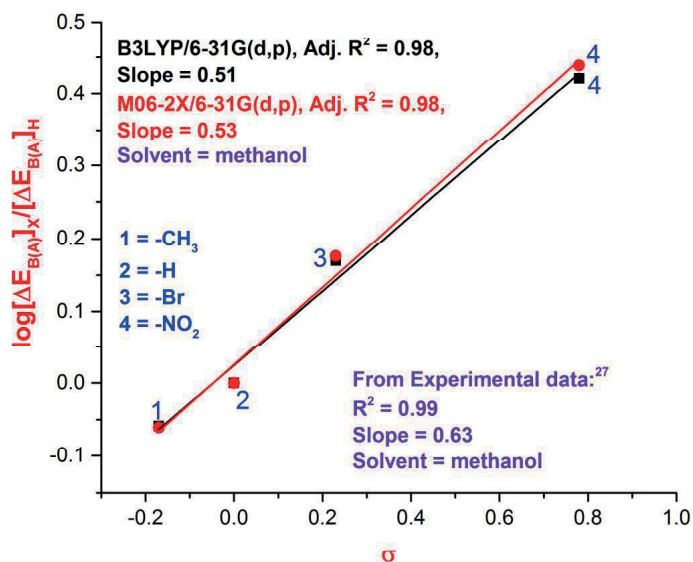


Figure 5.6. Plot of $\log \frac{[\Delta E_{B(A)}]_X}{[\Delta E_{B(A)}]_H}$ vs. σ for the reaction of para-substituted benzylbromides with diphenylamine at B3LYP/6-31G(d,p) and M06-2X/6-31G(d,p) levels of theory.

Table 5.3 (d). The values of σ^0 for different substituents and $\log \frac{[\Delta E_{B(A)}]_X}{[\Delta E_{B(A)}]_H}$ values for the reaction of para-substituted benzylbromide with diphenylamine in methanol at B3LYP/6-31G(d,p) and M06-2X/6-31G(d,p), levels of theory. -X is the substituent on the para-position of benzylbromide.

Entry	Substituent (-X)	σ^0	$\log \frac{[\Delta E_{B(A)}]_X}{[\Delta E_{B(A)}]_H}$	
			B3LYP/6-31G(d,p)	M06-2X/6-31G(d,p)
1	-CH ₃	-0.14	-0.059	-0.061
2	-H	0.00	0.000	0.000
3	-Br	0.26	0.170	0.176
4	-NO ₂	0.81	0.421	0.439

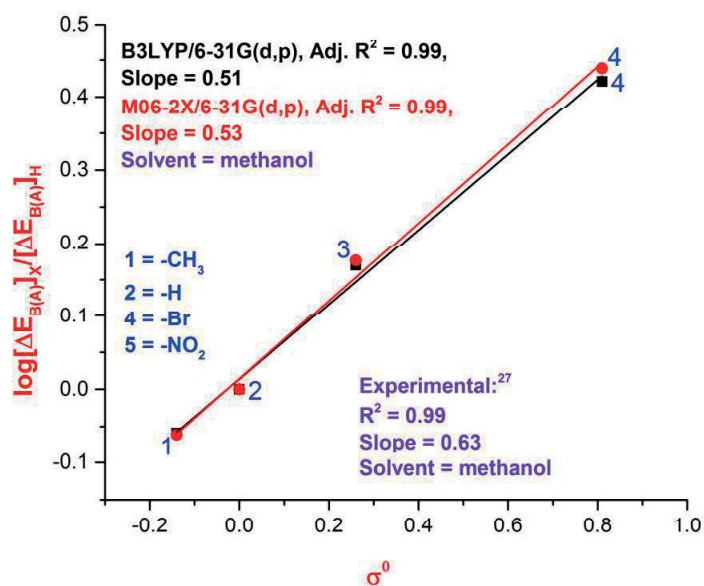


Figure 5.7. Plot of $\log \frac{[\Delta E_{B(A)}]_X}{[\Delta E_{B(A)}]_H}$ vs. σ^0 for the reaction of para-substituted benzylbromides with diphenylamine in methanol at B3LYP/6-31G(d,p) and M06-2X/6-31G(d,p) levels of theory.

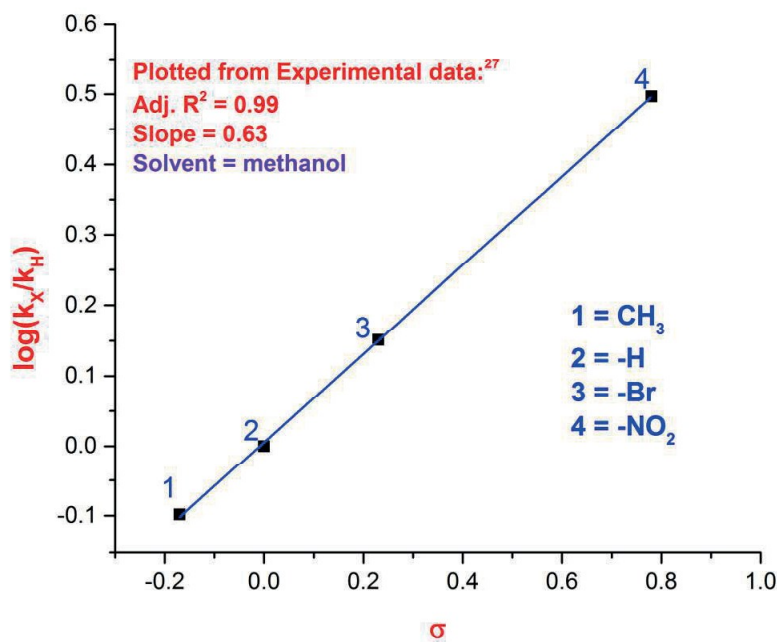


Figure 5.8. Plot of $\log \frac{k_X}{k_H}$ vs. σ for the reaction of para-substituted benzylbromides with diphenylamine generated from experimental data at 25 °C.²⁷

(d) Validation of DFRT based Hammett equation [equation (5.8)] for reactions (iv) – (vi):

Table 5.4 (a) represents the values of $\Delta E_{B(A)}$, $\Delta E_{A(B)}$ and $\Delta E_{SE(AB)}$ for the reaction of 2,2,2-trifluoroacetic acid with β -substituted ethanols [i.e., reaction (iv)].²⁸ Table 5.4 (b) contains the values of $\log \frac{[\Delta E_{B(A)}]_X}{[\Delta E_{B(A)}]_H}$ for the same reaction. The calculated values of ΔN [Table 5.4(c)] for the reaction of 2,2,2-trifluoroacetic acid with β -substituted ethanols [i.e., reaction (iv)]²⁸ confirm that 2,2,2-trifluoroacetic acid acts as an electron acceptor (A) while β -substituted ethanols act as electron donors (B) in all the cases and in both the methods. It is to be noted that -I substituted ethanol is not considered for correlation analysis as the basis set used for I atom is LANL2DZ, which is different from 6-31G(d,p) used for atoms of other substituents. Comparing the theoretically generated plots (Figure 5.9) with that of the experimentally generated one (Figure 5.10), it is clear that the nature of the plots are similar. The negative slopes of the plots indicate that the reaction is accelerated by electron donating substituents (unlike ionization of benzoic acid).

Table 5.4 (a). The values of $\Delta E_{B(A)}$, $\Delta E_{A(B)}$ and $\Delta E_{SE(AB)}$ (in kcal mol⁻¹) for the reaction of 2,2,2-trifluoroacetic acid with β -substituted ethanol at B3LYP/6-31G(d,p), LANL2DZ (For I atom) and M06-2X/6-31G(d,p), LANL2DZ (For I atom) levels of theory. Here, -X is the substituent on the β -position of ethanol.

Entry	-X	σ	B3LYP/6-31G(d,p), LANL2DZ (for I atom)			M06-2X/6-31G(d,p), LANL2DZ (for I atom)		
			$\Delta E_{B(A)}$	$\Delta E_{A(B)}$	$\Delta E_{SE(AB)}$	$\Delta E_{B(A)}$	$\Delta E_{A(B)}$	$\Delta E_{SE(AB)}$
1	-CH ₂ CH ₃	-0.05	10.62	-13.40	-2.78	11.21	-14.42	-3.21
2	-CH ₃	-0.04	10.74	-13.54	-2.80	11.25	-14.54	-3.30
3	-CH ₂ CH ₂ CH ₃	-0.03	10.80	-13.70	-2.90	11.50	-14.90	-3.40
4	-H	0.00	10.50	-13.30	-2.80	11.10	-14.20	-3.10
5	-OCH ₂ CH ₃	0.27	9.89	-11.70	-1.81	10.10	-12.50	-2.40
6	-I	0.39	5.40	-5.80	-0.40	5.90	-6.40	-0.50
7	-F	0.52	9.50	-10.2	-0.70	9.40	-11.23	-1.83
8	-NO ₂	0.76	7.74	-9.20	-1.46	8.20	-9.30	-1.10
9	-F ₃	1.56	6.70	-7.53	-0.83	7.40	-8.40	-1.00

Table 5.4 (b). The values of $\log \frac{[\Delta E_{B(A)}]_X}{[\Delta E_{B(A)}]_H}$ for the reaction of 2,2,2-trifluoroacetic acid with β -substituted ethanol at B3LYP/6-31G(d,p), LANL2DZ (For I atom) and M06-2X/6-31G(d,p), LANL2DZ (for I atom) levels of theory. Here, -X is the substituent on the β -position of ethanol.

Entry	-X	σ	B3LYP/6-31G(d,p), LANL2DZ (for I atom)	M06-2X/6-31G(d,p), LANL2DZ (for I atom)
			$\log \frac{[\Delta E_{B(A)}]_X}{[\Delta E_{B(A)}]_H}$	$\log \frac{[\Delta E_{B(A)}]_X}{[\Delta E_{B(A)}]_H}$
1	-CH ₂ CH ₃	-0.05	0.005	0.004
2	-CH ₃	-0.04	0.011	0.006
3	-CH ₂ CH ₂ CH ₃	-0.03	0.013	0.015
4	-H	0.00	0.000	0.000
5	-OCH ₂ CH ₃	0.27	-0.025	-0.041
6	-I	0.39	-0.288	-0.274
7	-F	0.52	-0.043	-0.072
8	-NO ₂	0.76	-0.132	-0.131

9	-F ₃	1.56	-0.195	-0.176
---	-----------------	------	--------	--------

Table 5.4 (c). Charge transfer (ΔN) values for the reaction of 2,2,2-trifluoroacetic acid with β -substituted ethanol at B3LYP/6-31G(d,p), LANL2DZ (for I atom) and M06-2X/6-31G(d,p), LANL2DZ (for I atom) levels of theory. -X is the substituent on β -position of ethanol. In all the cases 2,2,2-trifluoroacetic acid acts as an electron acceptor (A) and β -substituted ethanols as electron donors (B).

Entry	-X	σ	ΔN	
			B3LYP/6-31G(d,p), LANL2DZ (for I atom)	M06-2X/6-31G(d,p), LANL2DZ (for I atom)
1	-CH ₂ CH ₃	-0.05	0.13	0.14
2	-CH ₃	-0.04	0.13	0.14
3	-CH ₂ CH ₂ CH ₃	-0.03	0.14	0.15
4	-H	0.00	0.13	0.14
5	-OCH ₂ CH ₃	0.27	0.16	0.17
6	-I	0.39	0.05	0.06
7	-F	0.52	0.10	0.12
8	-NO ₂	0.76	0.01	0.02
9	-F ₃	1.56	0.07	0.08

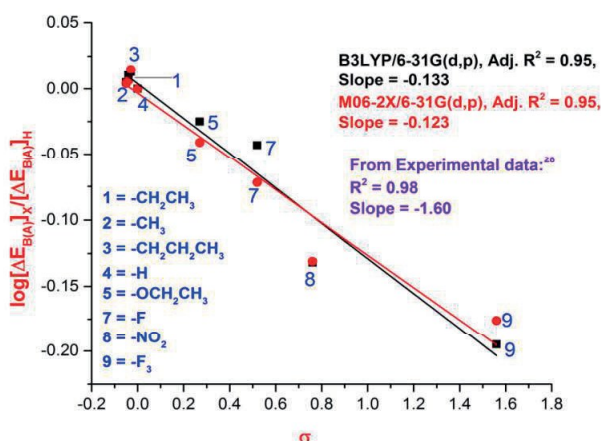


Figure 5.9. Plot of $\log \frac{[\Delta E_{B(A)}]_X}{[\Delta E_{B(A)}]_H}$ vs. σ for the reaction of 2,2,2-trifluoroacetic acid with β -substituted ethanols at B3LYP/6-31G(d,p) and M06-2X/6-31G(d,p) levels of theory.

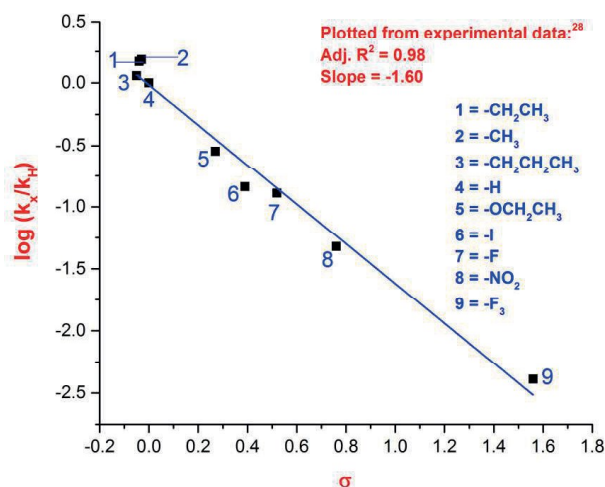


Figure 5.10. Plot of $\log \frac{k_x}{k_H}$ vs. σ for the reaction of 2,2,2-trifluoroacetic acid with β -substituted ethanols from experimental data at 25 °C.

Table 5.5 (a) represents the values of $\Delta E_{B(A)}$, $\Delta E_{A(B)}$ and $\Delta E_{SE(AB)}$ for the reaction of norbornene with *meta*-substituted arylazides [i.e., reaction (v)].²⁹ The substituent constant values used here are those of Exner's. Table 5.5 (b) contains the values of $\log \frac{[\Delta E_{B(A)}]_X}{[\Delta E_{B(A)}]_H}$ for the same reaction. The calculated values of ΔN [Table 5.5(c)] for the reaction of norbornene with *meta*-substituted arylazides [i.e., reaction (v)]²⁹ confirm that norbornene acts as an electron donor (B) while *meta*-substituted arylazides act as electron acceptors (A) in all the cases and in both the methods. Comparing the theoretically generated plot with that of the experimentally generated one i.e., Figures 5.11 and 5.12, respectively, it is evident that the nature of the plots are similar. The positive slopes of the plots confirm the electrophilic nature of *meta* substituted arylazides.

Table 5.5 (a). The values of $\Delta E_{B(A)}$, $\Delta E_{A(B)}$ and $\Delta E_{SE(AB)}$ (in kcal mol⁻¹) for the reaction of norbornene with meta-substituted arylazides in ethylacetate at B3LYP/6-31G(d,p) and M06-2X/6-31G(d,p) levels of theory. Here, -X is the substituent on the meta-position of arylazide.

Entry	-X	σ^0	B3LYP/6-31G(d,p)			M06-2X/6-31G(d,p)		
			$\Delta E_{B(A)}$	$\Delta E_{A(B)}$	$\Delta E_{SE(AB)}$	$\Delta E_{B(A)}$	$\Delta E_{A(B)}$	$\Delta E_{SE(AB)}$
1	-CH ₃	-0.07	6.34	-6.90	-0.56	6.30	-6.82	-0.52
2	-H	0.00	6.92	-7.70	-0.78	6.70	-7.40	-0.70
3	-OCH ₃	0.06	7.83	-8.90	-1.07	6.90	-8.30	-1.40
4	-Br	0.38	10.50	-12.60	-2.10	9.80	-11.85	-2.05
5	-NO ₂	0.70	22.10	-27.70	-5.60	19.80	-24.50	-4.70

Table 5.5 (b). The values of $\log \frac{[\Delta E_{B(A)}]_X}{[\Delta E_{B(A)}]_H}$ for the reaction of norbornene with meta-substituted arylazides in ethylacetate at B3LYP/6-31G(d,p) and M06-2X/6-31G(d,p) levels of theory. Here, -X is the substituent on the meta-position of arylazide.

Entry	-X	σ^0	B3LYP/6-31G(d,p)	M06-2X/6-31G(d,p)
			$\log \frac{[\Delta E_{B(A)}]_X}{[\Delta E_{B(A)}]_H}$	$\log \frac{[\Delta E_{B(A)}]_X}{[\Delta E_{B(A)}]_H}$
1	-CH ₃	-0.07	-0.038	-0.027
2	-H	0.00	0.000	0.000
3	-OCH ₃	0.06	0.054	0.013
4	-Br	0.38	0.181	0.165
5	-NO ₂	0.70	0.504	0.470

Table 5.5 (c). Charge transfer (ΔN) values for the reaction of norbornene with meta-substituted arylazides at B3LYP/6-31G(d,p) and M06-2X/6-31G(d,p), levels of theory. -X is the substituent on meta-position of arylazide. In all the cases norbornene acts as an electron donor (B) and meta-substituted arylazides act as an electron acceptors (A).

Entry	-X	σ^0	ΔN	
			B3LYP/6-31G(d,p), LANL2DZ (for I atom)	M06-2X/6-31G(d,p), LANL2DZ (for I atom)
1	-CH ₃	-0.07	0.09	0.04
2	-H	0.00	0.10	0.09
3	-OCH ₃	0.06	0.08	0.08
4	-Br	0.38	0.12	0.13
5	-NO ₂	0.70	0.70	0.73

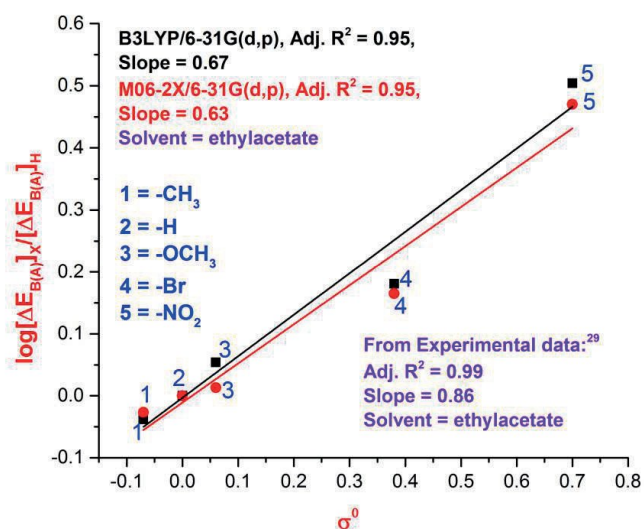


Figure 5.11. Plot of $\log \frac{[\Delta E_{B(A)}]_X}{[\Delta E_{B(A)}]_H}$ vs. σ^0 for the reaction of meta-substituted arylazides with norbornene at B3LYP/6-31G(d,p) and M06-2X/6-31G(d,p) levels of theory.

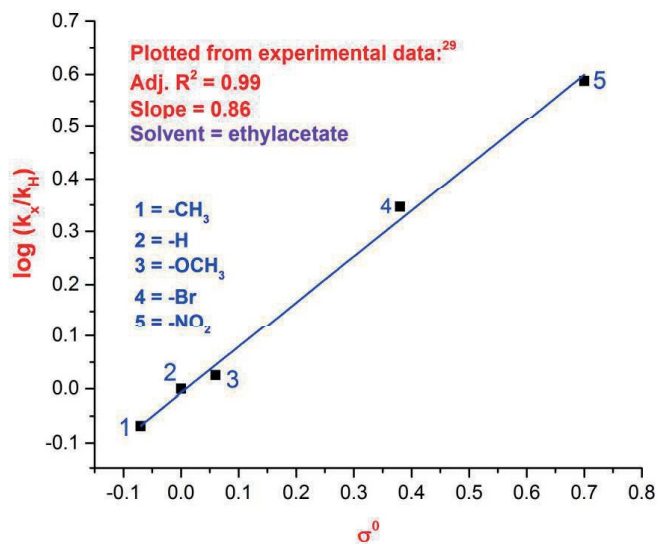


Figure 5.12. Plot of $\log \frac{k_X}{k_H}$ vs. σ^0 for the reaction of *meta*-substituted arylazides with norbornene from experimental data at 25 °C.

Table 5.6 (a) represents the values of $\Delta E_{B(A)}$, $\Delta E_{A(B)}$ and $\Delta E_{SE(AB)}$ for the reaction of norbornene with *para*-substituted arylazides [i.e., reaction (vi)].²⁹ The substituent constant values used here are those of Exner's. Table 5.6 (b) contains the values of $\log \frac{[\Delta E_{B(A)}]_X}{[\Delta E_{B(A)}]_H}$ for the same reaction. The calculated values of ΔN [Table 5.6 (c)] for the reaction of norbornene with *para*-substituted arylazides [i.e., reaction (vi)]²⁹ confirm that norbornene acts as an electron donor (B) while *para*-substituted arylazides act as electron acceptors (A) in all the cases and in both the methods. On Comparing the theoretically generated plot for this reaction with that of experimentally generated one i.e., Figures 5.13 and 5.14, respectively, it is evident that the nature of the plots are similar. The positive slopes of the plots confirm the electrophilic nature of *meta* substituted arylazides.

Table 5.6 (a). The values of $\Delta E_{B(A)}$, $\Delta E_{A(B)}$ and $\Delta E_{SE(AB)}$ (in kcal mol⁻¹) for the reaction of norbornene with para-substituted arylazides in ethylacetate at B3LYP/6-31G(d,p) and M06-2X/6-31G(d,p) levels of theory. Here, -X is the substituent on the para-position of arylazide.

Entry	-X	σ^0	B3LYP/6-31G(d,p)			M06-2X/6-31G(d,p)		
			$\Delta E_{B(A)}$	$\Delta E_{A(B)}$	$\Delta E_{SE(AB)}$	$\Delta E_{B(A)}$	$\Delta E_{A(B)}$	$\Delta E_{SE(AB)}$
1	-OCH ₃	-0.16	4.30	-4.47	-0.17	5.50	-5.96	-0.46
2	-CH ₃	-0.15	5.60	-6.10	-0.50	6.50	-7.01	-0.51
3	-H	0.00	6.92	-7.70	-0.78	6.70	-7.40	-0.70
4	-Br	0.26	8.30	-9.12	-0.82	8.80	-9.89	-1.09
5	-NO ₂	0.73	22.73	-28.63	-5.90	20.90	-27.60	-6.70

Table 5.6 (b). The values of $\log \frac{[\Delta E_{B(A)}]_X}{[\Delta E_{B(A)}]_H}$ for the reaction of norbornene with para-substituted arylazides in ethylacetate at B3LYP/6-31G(d,p) and M06-2X/6-31G(d,p) levels of theory. Here, -X is the substituent on the para-position of arylazide.

Entry	-X	σ^0	B3LYP/6-31G(d,p)	M06-2X/6-31G(d,p)
			$\log \frac{[\Delta E_{B(A)}]_X}{[\Delta E_{B(A)}]_H}$	$\log \frac{[\Delta E_{B(A)}]_X}{[\Delta E_{B(A)}]_H}$
1	-OCH ₃	-0.16	-0.206	-0.086
2	-CH ₃	-0.15	-0.092	-0.013
3	-H	0.00	0.000	0.000
4	-Br	0.26	0.079	0.118
5	-NO ₂	0.73	0.516	0.494

Table 5.6 (c). Charge transfer (ΔN) values for the reaction of norbornene with para-substituted arylazides at B3LYP/6-31G(d,p) and M06-2X/6-31G(d,p) levels of theory. Here, -X is the substituent on para-position of arylazide. In all the cases norbornene acts as an electron donor (B) and para-substituted arylazides act as electron acceptors (A).

Entry	-X	σ^0	ΔN	
			B3LYP/6-31G(d,p), LANL2DZ (for I atom)	M06-2X/6-31G(d,p), LANL2DZ (for I atom)
1	-OCH ₃	-0.16	0.05	0.05
2	-CH ₃	-0.15	0.08	0.10
3	-H	0.00	0.10	0.09
4	-Br	0.26	0.10	0.12
5	-NO ₂	0.73	0.28	0.33

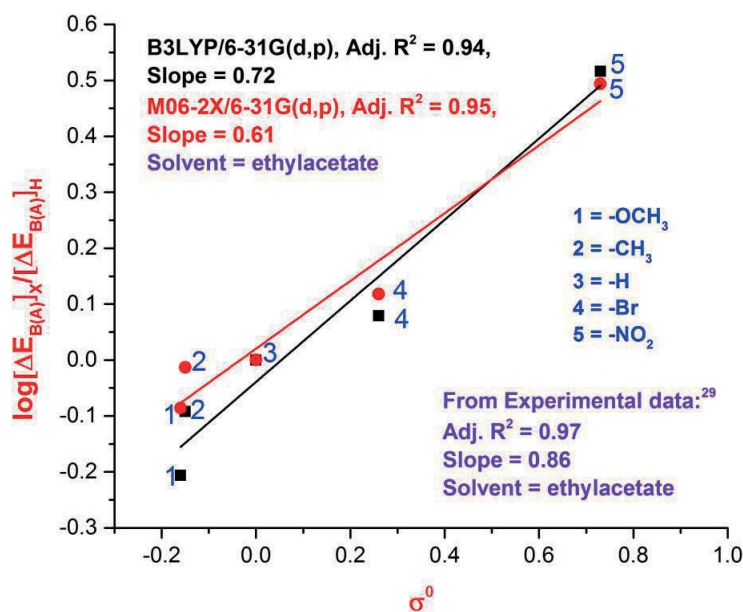


Figure 5.13. Plot of $\log \frac{[\Delta E_{B(A)}]_X}{[\Delta E_{B(A)}]_H}$ vs. σ^0 for the reaction of para-substituted arylazides with norbornene at B3LYP/6-31G(d,p) and M06-2X/6-31G(d,p) levels of theory.

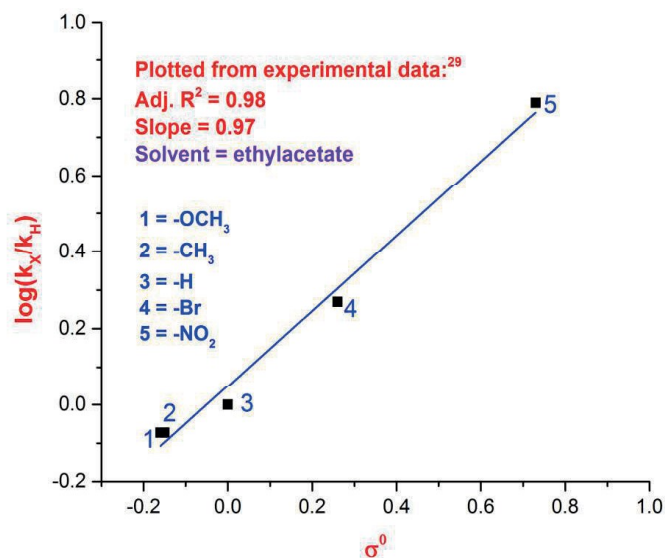


Figure 5.14. Plot of $\log \frac{k_X}{k_H}$ vs. σ^0 for the reaction of para-substituted arylazides with norbornene from experimental data at 25 °C.

5.5. Conclusions:

The analytical reasoning [sections 5.2(a) and 5.2(b)] and the generated data, contained in the present study, tries to validate Hammett's linear free energy relationship (i.e., $\log \frac{k_X}{k_H} = \rho\sigma$) through density functional reactivity theory (DFRT). The DFRT based (CDASE-scheme based, to be more specific) parameter used in place of rate constant, 'k', is the raising (i.e., positive) energy component $\Delta E_{B(A)}$ [equation (1.49)] of the overall stabilization energy, $\Delta E_{SE(AB)}$ [equation (1.48)].

DFRT modified Hammett's LFER [i.e., $\log \frac{[\Delta E_{B(A)}]_X}{[\Delta E_{B(A)}]_H} = \rho\sigma$] generates satisfactory results in all the six series of reactions chosen in the present study. Positive slopes (i.e., reaction constant, ρ) of the $\log \frac{[\Delta E_{B(A)}]_X}{[\Delta E_{B(A)}]_H}$ vs. σ (or σ^0) plots are indicative of the fact that para-substituted acetophenones, para-substituted benzylbromides, meta and para-substituted arylazides play the role of electrophilic reagents when reacted with hydroxylamine [reaction (i)],²⁵ diphenylamine [reaction (iii)]²⁷ and norbornene [reactions (v) and (vi)],²⁹ respectively. For the same reason it can be argued that the negative slope in the $\log \frac{[\Delta E_{B(A)}]_X}{[\Delta E_{B(A)}]_H}$ vs. σ plot for reactions (ii) and (iv) justify the

nucleophilic nature of para-substituted cumenes (except when X = -COCH₃) and β-substituted ethanols when reacted with dimethyldioxirane²⁶ and 2,2,2-trifluoroacetic acid, respectively.²⁸

Qualitatively similar reaction constants (i.e., ρ^0) values are obtained when $\log \frac{[\Delta E_{B(A)}]_X}{[\Delta E_{B(A)}]_H}$ are plotted against universal substituent constants (σ^0) of Exner.^{22,40} From the generated data and the nature of the plots using two different functionals (i.e., B3LYP and M06-2X), it can be argued that equation (5.8) (i.e., DFRT based Hammett equation) is independent of methods and basis sets used. The nature of the plots obtained either through $\log \frac{k_X}{k_H}$ vs. σ or through $\log \frac{[\Delta E_{B(A)}]_X}{[\Delta E_{B(A)}]_H}$ vs. σ is same and have almost equal correlation coefficient values (R^2 values) with similar type of slope.

It is to be noted here that experimental plots of $\log \frac{k_X}{k_H}$ vs. σ (or σ^0) were obtained at 25 °C (298.15 K) [except for reaction (i), where the plot between $\log \frac{k_X}{k_H}$ vs. σ was obtained at 22 °C (295.15 K)]. However, $\log \frac{[\Delta E_{B(A)}]_X}{[\Delta E_{B(A)}]_H}$ vs. σ (or σ^0) plots are obtained at 0 K for all the cases (as the DFRT based reactivity parameters are generated from quantum chemical calculations). Finally, the authors believe that DFRT based form of Hammett's LFER equation [equation (5.8)] can be used to get the initial idea of reaction mechanism before the actual experiment is carried out. This is possible because theoretically calculated $\Delta E_{B(A)}$ values can be used [equation (1.49)] instead of experimentally generated rate constant (k_X) values in the Hammett's LFER equation [equation (5.1) or (5.2)].

References:

1. R. G. Parr, R. G. Pearson, *J. Am. Chem. Soc.* **1983**, *105*, 7512.
2. R. T. Sanderson, *Science*. **1951**, *114*, 670.
3. R. T. Sanderson, *Science*. **1952**, *116*, 41.
4. R. G. Parr, R. A. Donnelly, M. Levy, W. E. Palke, *J. Chem. Phys.* **1978**, *68*, 3801.
5. P. Bagaria, S. Saha, S. M. V. Kavala, B. K. Patel, R. K. Roy. *Phys. Chem. Chem. Phys.* **2009**, *11*, 8306.
6. A. Sarmah, S. Saha, P. Bagaria, R. K. Roy, *Chem. Phys.* **2012**, *394*, 29.
7. A. Sarmah, R. K. Roy, *RSC Adv.* **2013**, *3*, 2822.
8. A. Sarmah, R. K. Roy, *J. Phys. Chem. C*. **2013**, *117*, 21539.
9. A. Sarmah, R. K. Roy, *J. Comput. Aided Mol. Des.* **2014**, *28*, 1153.
10. A. Sarmah, R. K. Roy, *J. Phys. Chem. C*. **2015**, *119*, 17940.
11. A. Sarmah, R. K. Roy, *Chem. Phys.* **2016**, *472*, 218.
12. A. Hamid, A. Anand, R. K. Roy, *Phys. Chem. Chem. Phys.* **2017**, *19*, 10905.
13. A. Hamid, R. K. Roy, *Int. J. Quantum Chem.* **2019**, *119*, e25909.
14. A. Hamid, R. K. Roy, *J. Phys. Chem. A*. **2020**, *124*, 1279.
15. L. P. Hammett, *J. Am. Chem. Soc.* **1937**, *59*, 96.
16. M. G. Evans, M. Polanyi, *Trans. Faraday Soc.* **1935**, *31*, 875.
17. M. G. Evans, M. Polanyi, *Trans. Faraday Soc.* **1936**, *32*, 1333.
18. H. H. Jaffé, *Chem. Rev.* **1953**, *53*, 191.
19. C. Hansch, A. Leo, R. W. Taft, *Chem. Rev.* **1991**, *91*, 165.
20. R. K. Akhiani, M. I. Moore, J. G. Pribyl, S. L. Wisnu. *J. Org. Chem.* **2014**, *79*, 2384.
21. S. L. Keenan, K. P. Peterson, K. Peterson, K. Jacobson, *J. Chem. Educ.* **2008**, *85*, 558.
22. O. Exner, J. Lakomy, *Coll. Czech. Chem. Commun.* **1970**, *35*, 1371.
23. P. Geerlings, F. De. Proft, W. Langenaeker, *Chem. Rev.* **2003**, *103*, 1793.
24. S. Pal, R. K. Roy, A. K. Chandra, *J. Phys. Chem.* **1994**, *98*, 2314.
25. R. J. Mullins, A. Vedernikov, R. Viswanathan, *J. Chem. Educ.* **2004**, *81*, 1357.
26. R. W. Murray, Hong. Gu, *J. Org. Chem.* **1995**, *60*, 5673.
27. S. R. Reddy, P. Manikyamba, *J. Chem. Sci.* **2006**, *118*, 257.
28. J. B. Smith, H. Byrd, S. E. O'Donnell, W. Davis, *J. Chem. Educ.* **2010**, *87*, 845.

-
29. P. Scheiner, J. H. Schomaker, S. Deming, W. J. Libbey, G.P. Nowack, *J. Am. Chem. Soc.* **1964**, *87*, 307.
 30. M. J. Frisch, et al. Gaussian 09 Rev. D.01, Gaussian INC.: Wallingford, CT, **2013**.
 31. A. D. Becke, *J. Chem. Phys.* **1993**, *98*, 5648.
 32. C. T. Lee, W. T. Yang, R. G. Parr, *Phys. Rev. B.* **1988**, *37*, 785.
 33. W. J. Hehre, R. F. Stewart, J. A. Pople, *J. Chem. Phys.* **1969**, *51*, 2657.
 34. Y. Zhao, D. G. Truhlar, *Theor. Chem. Acc.* **2008**, *120*, 215.
 35. P. J. Hay, W. R. Wadt, *J. Chem. Phys.* **1985**, *82*, 299.
 36. C. E. Check, T. O. Faust, J. M. Bailey, B. J. Wright, T. M. Gilbert, L. S. Sunderlin, *J. Phys. Chem. A.* **2001**, *105*, 8111.
 37. M. Walker, A. J. A. Harvey, A. Sen, C. E. H. Dessent, *J. Phys. Chem. A.* **2013**, *117*, 12590.
 38. B. Mennucci, E. Cancès, J. Tomasi, *J. Phys. Chem. B.* **1997**, *101*, 10506.
 39. A. V. Marenich, C. J. Cramer, D. G. Truhlar, *J. Phys. Chem. B.* **2009**, *113*, 6378.
 40. O. Exner, S. Bohm, *J. Org. Chem.* **2002**, *67*, 6320.



This document was created with the Win2PDF "print to PDF" printer available at <http://www.win2pdf.com>

This version of Win2PDF 10 is for evaluation and non-commercial use only.

This page will not be added after purchasing Win2PDF.

<http://www.win2pdf.com/purchase/>